Journal of Petroleum Research and Studies

Open Access
No. 34 part 2, April 2022, pp. 302-315

P- ISSN: 2220-5381
E- ISSN: 2710-1096

DOI: http://doi.org/10.52716/jprs.v12i1(Suppl.).639

Optimizing of Turbine blade spar using Ansys program

Firas Thair Al-Maliky[1,*], Dhurgham A. Kadhim[2]
[1]University of Alkafeel, Computer Engineering Techniques, Najaf, Iraq
[2]KRP (Karbala Refinery Project)
[*]Corresponding Author E-mail: firas.almaliky@alkafeel.edu.iq, firasthair@gmail.com
[2]durghamalshakerchi@gmail.com

6th Iraq Oil and Gas Conference, 29-30/11/2021

Abstract

The current work involved optimizing the spars of wind turbine blades while taking into account the wind speed quantities that affected the blade structure. The objective was to determine the optimal dimensions of turbine blade spar configurations using the finite element method under the influence of the maximum pressure associated with the first mode shape while maintaining the Von Misses stresses within the assumed safety factor (1.5). (200-230 MPa). The blade was stiffened with a main box spar and two auxillary spars on each side. Appropriate spar locations were specified for poisons with a high natural frequency first mode. The blade parts' dimensions were discretized to allow for greater flexibility and precision in dimension assignment. By utilizing the ANSYS program, the optimization process required a certain number of iterations to modify the blade structure's dimensions. Optimized iteration was considered in order to increase the thickness in areas of high stress and decrease the thickness in areas of low stress. Additionally, a comparison between a blade structure with optimal dimensions and one with non-optimal dimensions was included.

Keywords: Spar, ansys, feasible design.

1. Introduction:

The Optimization is a strategy for determining the optimal design. By "optimal design," we mean one that satisfies all specified requirements while incurring the fewest possible costs in terms of weight, surface area, volume, stress, and cost. In other words,

Open Access
No. 34 part 2, April 2022, pp. 302-315
P- ISSN: 2220-5381
E- ISSN: 2710-1096

the optimal design is typically the most effective. The ANSYS program includes a variety of optimization methods that may be used to solve a wide variety of optimization problems. These approaches can be applied quickly to the majority of engineering problems. One of these ways is the first order method, which is more suitable for issues requiring high accuracy because it is based on design sensitivity. While attempting to achieve the optimal design, the ANSYS optimization procedures make use of three distinct types of variables to represent the design process: design variables, state variables, and the objective function.THEORY The independent variables in an optimization analysis are the design variables. The vector of design variables is indicated by:

$x = \lfloor x_1\ x_2\ x_3\ \ldots . x_n \rfloor$ ..... (1)

Design variables are subject to n constraints with upper and lower limits [1], that is,

$\underline{x_i} \leq \overline{x_i} \quad (i = 1,2,3, \ldots \ldots n)$.....(2)

The design variable constraints are often referred to as side constraints and define what is commonly called feasible design space.

Now, minimize

$f = f(x)$ ..... (3)

subject to

$g_i(x) \leq \overline{g_i} \quad (i = 1,2,3 \ldots m_1)$ .....(4)

$\underline{h_i} \leq h_i(x) \quad (i = 1,2,3, \ldots m_2)$ .....(5)

$\underline{w_i} \leq w_i(x) \leq \overline{w_i} (i = 1,2,3, \ldots m_3)$.....(6)

where:

f = objective function

g_i, h_i, w_i = state variables containing the design, with under bar and over bars representing lower and upper bounds respectively[2].

State variables are also known as dependent variables since they vary in relation to the vector x of design variables[3]. Equations (3) through (6) denote a constrained minimization problem whose objective is to minimize the objective function f while adhering to the limitations imposed by Equations (2), (4), (5), and (6).

Open Access
No. 34 part 2, April 2022, pp. 302-315
P- ISSN: 2220-5381
E- ISSN: 2710-1096

2. FEASIBLE VERSUS INFEASIBLE DESIGN SETS

The term "feasible designs" refers to design configurations that satisfy all constraints[4]. Infeasible configurations are those that have one or more violations. Each state variable limit is given a tolerance when determining the feasible design space. Therefore, if x* is a specified design set defined as:

$x^* = (x_1^* \, x_2^* \, x_3^* \, \dots \dots \, x_n^*)$ ……..…(7)

The design is deemed feasible only if

$g_i^* = g_i(x^*) \leq \overline{g_i} + \alpha_i \;\; (i = 1,2,3, \dots m_1)$[5]…….(8)

$\underline{h_i} - \beta_i \leq h_i^* = h_i(x^*) \;\; (i = 1,2,3, \dots m_2)$… ……...…..... (9)

$\underline{w_i} - \gamma_i \leq w_i^* = w_i(x^*) \leq \overline{w_i} + \gamma_i (i = 1,2,3, \dots m_3)$ ……. (10)

and

$\underline{x_i} \leq x_i^* \leq \overline{x_i} (i = 1,2,3, \dots n)$ … … … … … … … … … … … … … … ….(11)

Equation (8) to Equation (11), are the defining statements of a feasible design set in the ANSYS optimization routines [6].

3. THE BEST DESIGN SET

Due to the fact that tools generate design sets and an objective function is given, the better design set is computed and its number is stored. The optimal set is determined in one of the following circumstances. If there are multiple viable sets, the optimal design set is the one with the lowest objective function value. In other words, it is the set that conforms most closely to the mathematical objectives represented in Equations (3) through (8). If all design sets are infeasible, the best design set is the one that is the closest to being feasible, regardless of the value of the objective function [7].

The following parameters were taken into account throughout the optimization process: As indicated in Figure (1), the blade was strengthened by a primary box spar, two axillary spars on the left and right sides of the blade, and ribs in each sector of the blade. The sites of suitable spars were determined using poisons with a high natural frequency in the first mode[8] and [9].

Open Access
No. 34 part 2, April 2022, pp. 302-315
P- ISSN: 2220-5381
E- ISSN: 2710-1096

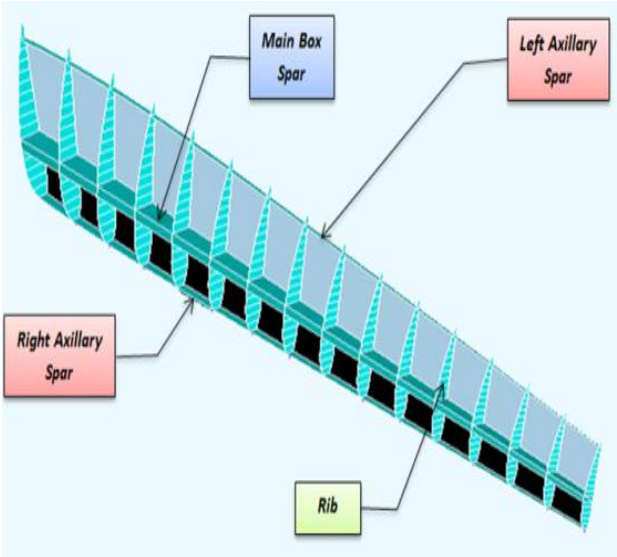

Fig. (1) Box spar, Axillary spars and Rib of blade structure without skin.

According to the yield stress of Aluminium-2024-T4 (_y=324 MPa), the allowed Von Misses stress was considered to be not more than (230 MPa) and not less than (200 MPa). The value of stress in the low stress zone was omitted due to the low magnitude of the affecting loads in this region. Their thickness is stated in terms of the aluminum sheet's threshold thickness (minimum sheet plate thickness of AL-2024-T4= 0.1 mm) [10] were discretized to allow for greater flexibility and precision when allocating measurements. Skin (1), skin (2), skin (3), and skin (4) were separated from the blade skin. Each portion was subdivided into five regions (A, B, C, D, and E), as seen in Figures (2) and (3).

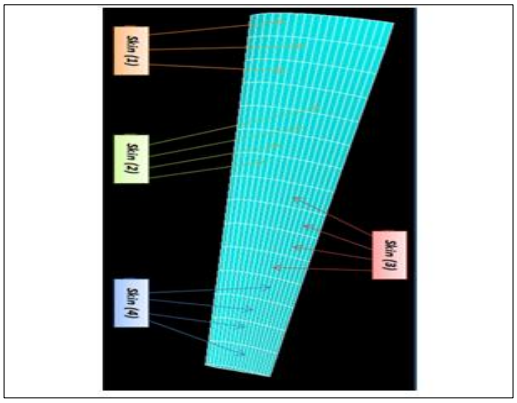

Fig. (2): The blade skin parts.

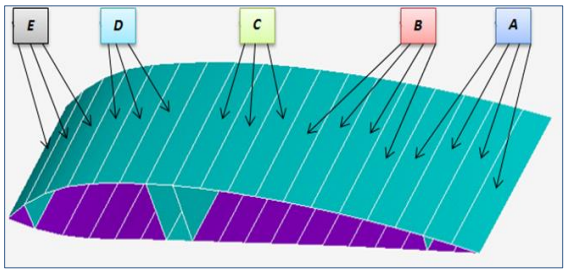

Fig. (3): Section of blade shows the skin region.

Open Access
No. 34 part 2, April 2022, pp. 302-315
P- ISSN: 2220-5381
E- ISSN: 2710-1096

The two sides' axillary spars were discretized into four components (ASP (1), ASP (2), ASP (3), and ASP (4)). The rib was divided into four segments (RIB 1, RIB 2, RIB 3, and RIB 4). The main box spar was subdivided into fifteen components (MBSP (1), MBSP (2), MBSP (3), MBSP (4), MBSP (5), MBSP (15)). As seen in Figure (4). The dimensions of the blade components were initially considered to be uniform (1mm) in thickness.

The highest pressure PSD load from the first mode was applied to the structure's lower surface. The highest pressure PSD load from the first mode was applied to the structure's lower surface. Static analysis was performed, and the results of stress calculations were computed.

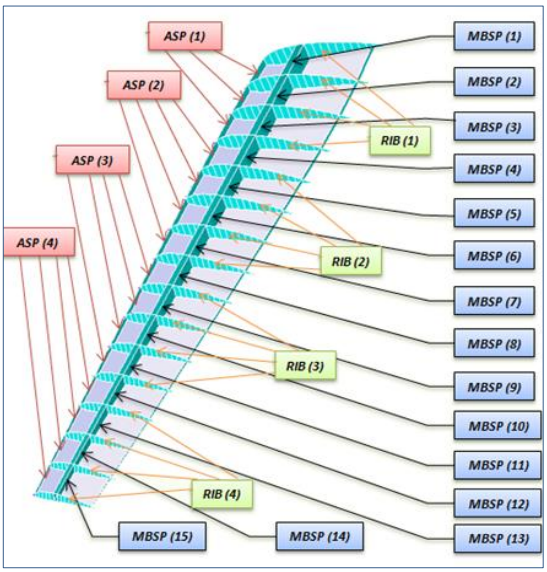

Fig. (4): The parts of axillary spars, Main box spar and Ribs.

4. RESULTS AND DISSCUSSION

The optimization technique requires a certain number of iterations to alter the blade structure's dimension. Optimize iteration was explored in order to raise the thickness in areas of high stress and decrease the thickness in areas of low stress. Tables (1) and (2) show the final optimized dimensions of the blade thicknesses in each section (2).

Open Access
No. 34 part 2, April 2022, pp. 302-315
P- ISSN: 2220-5381
E- ISSN: 2710-1096

Table (1) The skin, rib and axillary spars dimension parts.

Region	PART(1)	PART(2)	PART(3)	PART(4)
SKA(mm)	0.27	0.25	0.23	0.2
SKB(mm)	0.3	0.27	0.22	0.22
SKC(mm)	0.35	0.3	0.27	0.22
SKD(mm)	0.4	0.3	0.27	0.13
SKE(mm)	0.35	0.28	0.12	0.1
ASP(mm)	0.2	0.18	0.17	0.15
RIB(mm)	0.3	0.28	0.26	0.22

Table (2) Main box spar dimension parts.

MBSP(mm)	MBSP(1)	MBSP(2)	MBSP(3)	MBSP(4)	MBSP(5)	MBSP(6)	MBSP(7)	MBSP(8)	MBSP(9)	MBSP(10)	MBSP(11)	MBSP(12)	MBSP(13)	MBSP(14)	MBSP(15)
	2.1	1.8	1.3	1.25	1	0.8	0.6	0.4	0.2	0.18	0.18	0.15	0.15	0.1	0.1

The results of the analysis of optimized and non-optimized blades were compared. The thickness of this unoptimized blade is constant throughout the blade construction (0.8 mm). The permitted Von Misses stress cannot exceed (230 MPa) and must be less than (200 MPa) based on the yield stress of Aluminium-2024-T4 (_y=324 Pa).

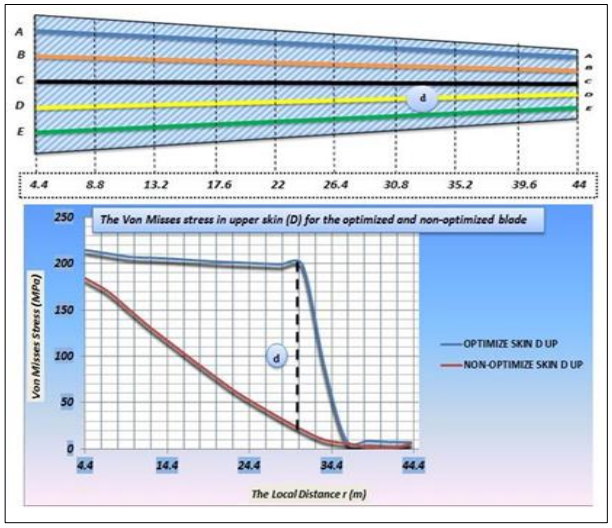

Fig. (5): Von Misses stress in upper skin (D) for optimized and non-optimized blade.

Open Access
No. 34 part 2, April 2022, pp. 302-315
P- ISSN: 2220-5381
E- ISSN: 2710-1096

From part (D), the reduction in weight was obtained by (63%) percent where the thickness decreased from $(t_{non\ optimize} = 0.8mm \rightarrow t_{optimize} = 0.275mm)$ and the results showed high amount of stress approaching to the limits of safety.

For example, the amount of stress in point (d) on non-optimized upper skin (D) was $(\sigma_{non\ optimize} = 21.21$ MPa) and then became $(\sigma_{optimize} = 198.43$ MPa) on optimized upper skin (D) with a reduction in weight by (66.3%)percent. It was observed the same thing in regions (A, B, C and E) of upper skin as shown in Table (3). The weight in upper skin structure was $(W_{non\ optimize} = 3416.5\ N)$ and then became $(W_{optimize} = 1357.2\ N)$ where the stress approached the limits of safety.

Table (3) The thickness and weight reduction in the in the upper skin of blade.

Skin	Thickness Reduction $(t_{non\ optimize} \rightarrow t_{optimize})mm$	The Percentage of weight reduction $\left(\frac{W_{non\ optimize} - W_{optimize}}{W_{non\ optimize}}\right)100\%$
A	(0.8 → 0.24)mm	68.75%
B	(0.8 → 0.253)mm	65.3%
C	(0.8 → 0.285)mm	62.4%
E	(0.8 → 0.213)mm	72.4%

Figures (6, 7, and 8) represent the stress distribution in skin (A, B, C and E) respectively for optimized and non-optimized structure of upper blade skin.

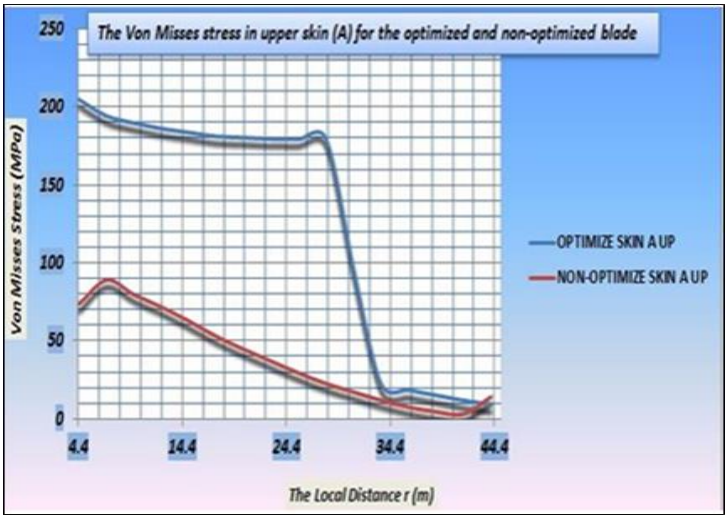

Fig. (6): Von Misses stress in upper skin (A) for optimized and non-optimized blade

Open Access
No. 34 part 2, April 2022, pp. 302-315
P- ISSN: 2220-5381
E- ISSN: 2710-1096

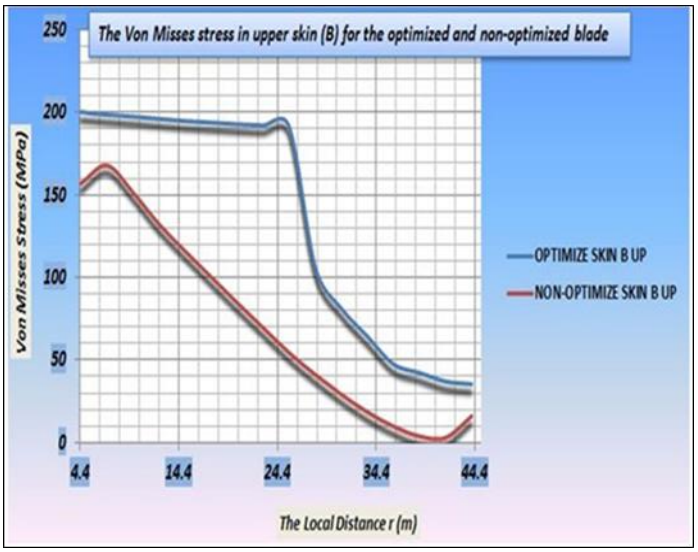

Fig. (7): Von Misses stress in upper skin (B) for optimized and non-optimized blade.

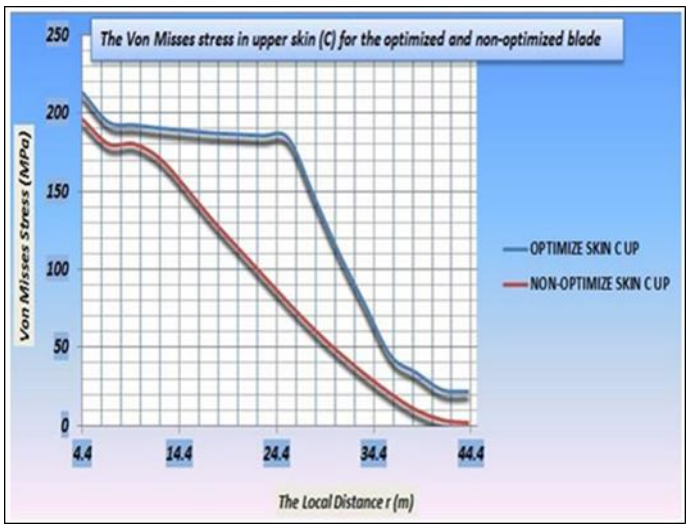

Fig. (8): Von Misses stress in upper skin (C) for optimized and non-optimized blade.

In lower skin surface, the stress distribution in region (B) for optimized and non-optimized structure was indicated in Figure (9).

Open Access
No. 34 part 2, April 2022, pp. 302-315
P- ISSN: 2220-5381
E- ISSN: 2710-1096

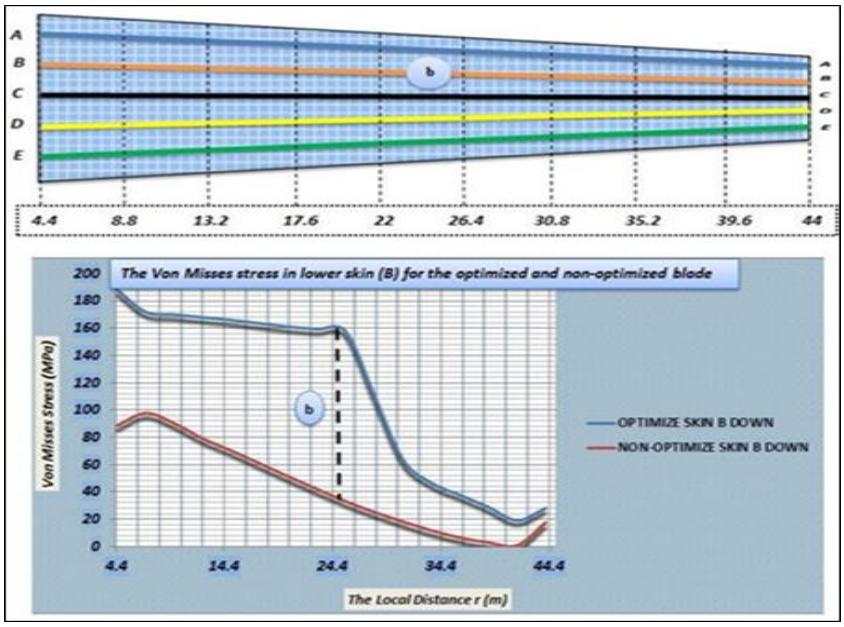

Fig. (9): Von Misses stress in lower skin (B) for optimized and non-optimized blade.

From part (B), the reduction in weight was obtained by (65.3%) percent where the thickness decreased from ($t_{non\ optimize} = 0.8mm \rightarrow t_{optimize} = 0.253mm$) and the results showed high amount of stress approaching to the limits of safety. For example, the amount of stress in point (b) on non-optimized lower skin (B) was ($\sigma_{non\ optimize} = 33.196\text{MPa}$) and then became ($\sigma_{optimize} = 158.135\text{MPa}$) on optimized lower skin (B) with a reduction in weight by (66%)percent.

The reduction in weight and thickness for regions (A, B, C and E) in lower skin was the same in upper skin because the blade skin was symmetrical in the upper and lower sides. Figures (10, 11, 12 and 13) represent the stress distribution in skin (A, C, D and E) respectively for optimized and non-optimized structures of lower skin surface.

Open Access
No. 34 part 2, April 2022, pp. 302-315
P- ISSN: 2220-5381
E- ISSN: 2710-1096

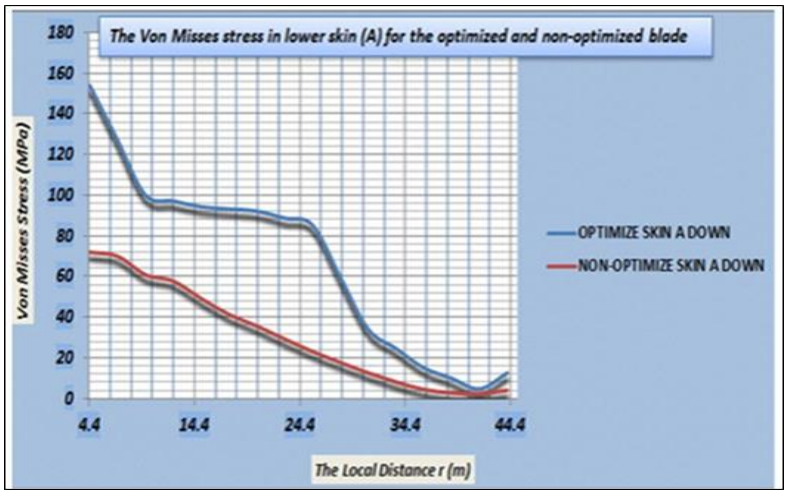

Fig. (10): Von Misses stress in lower skin (A) for optimized and non-optimized blade

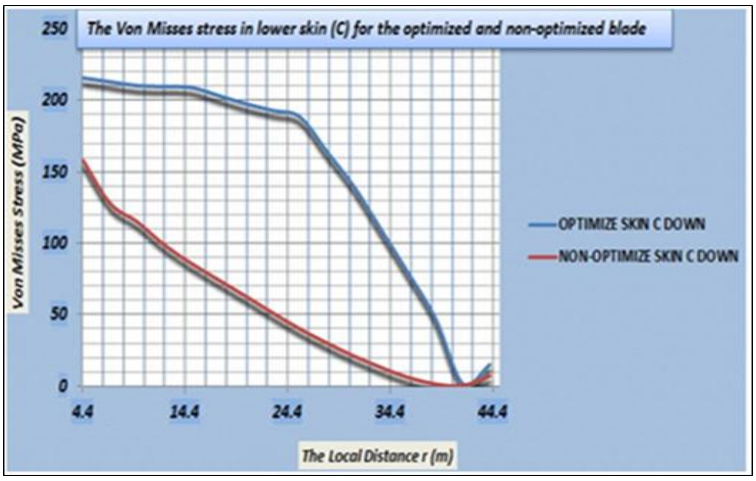

Fig. (11): Von Misses stress in lower skin (C) optimized and non-optimized blade.

Fig. (12): Von Misses stress in lower skin (D) for optimized and non-optimized blade.

Open Access
No. 34 part 2, April 2022, pp. 302-315
P- ISSN: 2220-5381
E- ISSN: 2710-1096

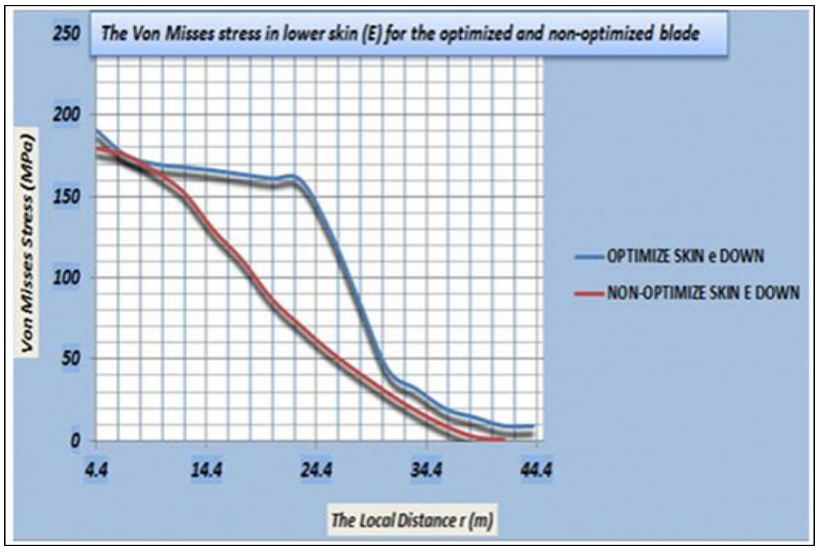

Fig. (13): Von Misses stress in lower skin (E) for optimized and non-optimized blade

The stress distribution in main box spar, left spar and right spar for optimized and non-optimized structures were indicated in Figure (14) respectively. In the main box spar, the reduction in weight was obtained by (33.4%) percent where the thickness decreased from ($t_{non\ optimize} = 0.8mm \rightarrow t_{optimize} = 0.68mm$). For example, the amount of stress in point (a) on non-optimized main box spar was ($\sigma_{non\ optimize} = 21.561$MPa) and then became ($\sigma_{optimize} = 185.497$MPa) on main box spar with a reduction in weight by (75%)percent.

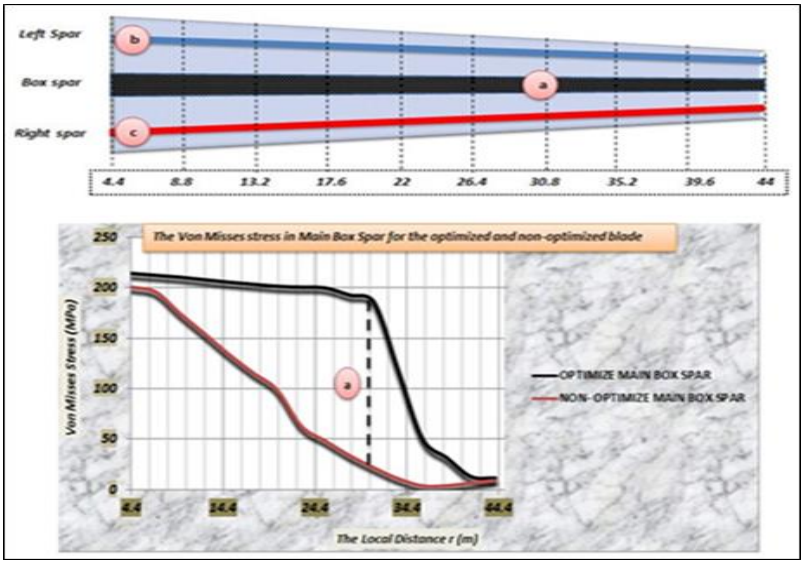

Fig. (14): Von Misses stress in main box spar for optimized and non-optimized blade

Open Access
No. 34 part 2, April 2022, pp. 302-315
P- ISSN: 2220-5381
E- ISSN: 2710-1096

It was observed the same thing in the left and right spars and the results of weight and thickness reduction were indicated in Table (4).

Table (4) The thickness and weight reduction in the in the left and right spars.

Spar	**Thickness Reduction** $(t_{non\ optimize} \rightarrow t_{optimize})mm$	**The Percentage of weight reduction** $\left(\frac{W_{non\ optimize} - W_{optimize}}{W_{non\ optimize}}\right)100\%$
Left	$(0.8 \rightarrow 0.175)$mm	**78%**
Right	$(0.8 \rightarrow 0.175)$mm	**78%**
Region	**Stress reduction** $(\sigma_{non\ optimize} \rightarrow \sigma_{optimize})MPa$	**The Percentage of weight reduction**
B	$(43.06 \rightarrow 183.7)MPa$	94.5%
c	$(22.7 \rightarrow 99.413)MPa$	73.4%

5. CONCLUSION

The stress distribution along optimized blade structures was shown to be more stable at high stress levels until it reached the threshold area, after which the stress continued to fall until it reached the blade's tip. In non-optimized structures, stress is noted to be greatest at the blade's root and gradually decreases until it reaches the blade's tip. The total weight of the non-optimized blade was (8348.3 N), which was reduced to (3545.5 N) for the improved blade (57.53 percent). Additionally, the natural frequency in the first mode was (0.675 Hz) for the non-optimized structure and became (0.97 Hz) for the improved structure. This demonstrates that the optimized blade was stiffer than the non-optimized blade, where the natural frequency is proportional to the root of the blade's stiffness and inversely proportional to the root of the blade's mass.

Open Access
No. 34 part 2, April 2022, pp. 302-315
P- ISSN: 2220-5381
E- ISSN: 2710-1096

References

[1] *Wang Xudong*[1,2], *Wen Zhong Shen*[1], *Wei Jun Zhu*[1], *Jens Nørkaer Sørensen*[1] *and Chen Jin*[2], "Blade Optimization for Wind Turbines", [1]Department of Mechanical Engineering, Technical University of Denmark, DK-2800 Lyngby, Denmark, [2]State Key Laboratory of Mechanical Transmission, Chongqing University, Chongqing, China, 2009.

[2] *Jie ZHU*[a], *Xin CAI*[a,b], *Pan PAN*[a] *and Rongrong GU*[a], "Optimization design of spar cap layup for wind turbine Blade", [a]College of Mechanics and Materials, Hohai University, Nanjing 210098, China, [b]College of Water Conservancy and Hydropower Engineering, Hohai University, Nanjing 210098, China, 2012.

[3] *Xin Cai*[1,2], *Jie Zhu*[1], *Pan Pan*[1] *and Rongrong Gu*[1], "Structural Optimization Design of Horizontal-Axis Wind Turbine Blades Using a Particle Swarm Optimization Algorithm and Finite Element Method", [1]College of Mechanics and Materials, Hohai University, Nanjing 210098, China; E-Mails: xcai@hhu.edu.cn (X.C.); panpan.159@163.com (P.P.); gurr99@126.com (R.G.) [2]College of Water Conservancy and Hydropower Engineering, Hohai University, Nanjing 210098, China, 2012.

[4] *Gaetan Kenway and Joaquim R. R. A. Martinsy*, "Aerostructural Shape Optimization of Wind Turbine Blades Considering Site-Specific Winds", University of Toronto Institute for Aerospace Studies, Toronto, Ontario, Canada, M3H 5T6, 2008.

[5] *J.S. Rao*[1], *Bhaskar Kishore*[2] *and Vasantha Kumar*[3], "Weight Optimization of Turbine Blades", [1]Chief Science Officer, Altair Engineering, [2]Project Engineer, Altair Product Design, [3]Project Manager, Altair Product Design, 2011.

[6] *Wen-Bin Young*, "Optimization of the skin thickness distribution in the composite wind turbine blade", Dept. of Aeronaut & Astronaut, Nat. Cheng Kung Univ, Tainan, Taiwan, 2011, pp.62-66.

[7] *Box, G.E.P., Hunter, W.G. and Hunter, J.S.*, "Statistics for Experimenters", John Wiley & Sons, Chapter 10, 1978.

Open Access
No. 34 part 2, April 2022, pp. 302-315
P- ISSN: 2220-5381
E- ISSN: 2710-1096

[8] ***Tae gyun (Tom) Gwon,*** **"**Structural Analyses of Wind Turbine Tower for 3KW Horizontal Axis Wind Turbine", *California Polytechnic State University, San Luis Obispo* Follow, 2011.

[9] *Pabut, O., Allikas, G., Herranen, H., Talalaev, R. & Vene, K,* "Model Validation and Structure Analysis of A Small Wind Turbine Blade", International DAAAM Baltic Conference, INDUSTRIAL ENGINEERING, 2012.

[10] *Zhengzhou Zhongxin Aluminum and Cable,* "top quality 2024 aluminum sheet manufactures", China (Mainland),

http://www.alibaba.com/productgs/569418181/top_quality_2024_aluminum_shee_metal.html., 2012.